

INFLUENCE OF SINTERING CONDITIONS ON RESISTANCE OF METALLIZATION FOR SILICON SOLAR CELLS

MOJROVÁ Barbora^{1*}, BUCK Thomas²

¹*Department of Microelectronic, Faculty of Electrical Engineering and Communication, Brno University of Technology, Brno, Czech Republic, EU*

²*International Solar Energy Research Center Konstanz, Konstanz, Germany, EU*

* xmojro00@stud.feec.vutbr.cz

Abstract

Contact formation is one of the significant steps, which have to be optimized in the production of silicon solar cells with high efficiency based on N-type substrates. In this work a comparison of the effect of various sintering conditions on the contact formation process was done. Contacts were screen printed on passivated boron doped P⁺ emitters using two pastes for front-side metallization from different producers. Two different temperature profiles were compared at an atmospheric concentration of O₂. The influence of the O₂ concentration on resistance was investigated for one profile. Resistance changes during firing were measured simultaneously with the temperature using Rapid Thermal Processes (RTP) modified to in-situ resistance measurement.

Keywords: Silicon solar cell, metallization, contacts formation

1. INTRODUCTION

Solar cell metallization is one of the major efficiency limiting and cost determining steps in solar cell processing. Two main loss mechanisms are related to the metallization, optical shading losses and electrical series resistance losses. There are lots of different methods of producing solar cell metallization depending on cells structure. However, the most of producers of silicon solar cell used metallization based on screen printing and contact firing using RTP process due to its simplicity, high throughput, and a price. Due to the short firing cycles used, sintering kinetics gain a huge impact on the microstructure formation. [1, 2, 3, 4].

1.1. Process of contact formation

Usually the screen printing metallization comprises back contacts printing and drying, front contacts printing and drying, and firing. The printed contacts are dried to obtain higher stability of the print by eliminating humidity before firing. High temperature during firing is necessary to open an antireflection (ARC) and passivation layer (e.g. silicon oxide SiO_x, silicon nitride SiN_x) and to support the reactions in the course of firing. The silver mass transport and viscous flow of the glass is crucial for the contact formation. The simplified model of contact formation is shown in the **Fig. 1**. During the firing, the organic ingredients of the paste are thermally decomposed, the glass frit melts and wets the wafer surface. The antireflection and passivation layer is etched by the fluidized glass frit, which gets into direct contact with substrate. In the process, excess silver (Ag) particles as well as etched Si are dissolved in the glass frit. During the peak zone, where the wafer is heated within seconds up to peak temperature U_{peak} typically ranging between 800 °C to 950 °C, the actual contact formation occurs. The cooling is usually as fast as the heating process. Upon cooling down from the firing peak, the excess Si contained in the glass frit recrystallizes epitaxially on the substrate, and crystallites start to grow randomly on the Si surface to form an electrical contact with the emitter. At optimal firing conditions the crystallites grow in epitaxial relation with Si. Finally the glass frit layer solidifies as a quasicontinuous layer above the Si and the interface crystallites. The current conduction in the solar cell proceeds via small silver crystallites and colloidal precipitates, which are formed in the interface layer between the silver track and the silicon during the short firing step and via the sintered silver tracks [1, 4, 5, 6, 7, 8].

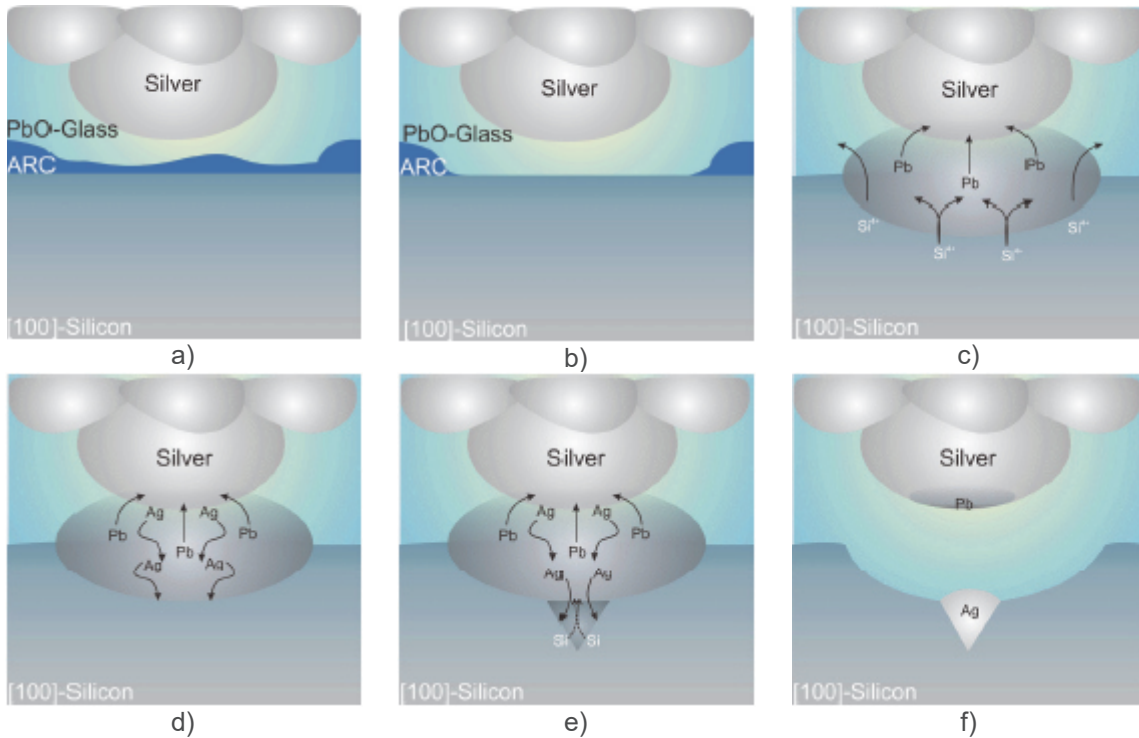


Fig. 1 Simplified model of contact formation: a) schematic cross section of Ag thick film paste on [100] Si after combustion of organics; b) glass etches through SiN_x layer; c) redox reaction between Si and glass, lead (Pb) is formed; d) liquid Pb starts to melt Ag; e) Ag - Pb melt reacts with Si, inverted pyramids are formed; f) on cooling down Ag recrystallises on (111)-Si planes [5]

1.2. In-situ resistance measurement

The measurement of the contact resistance during the firing step (in-situ resistance measurement) has a high potential to examine the ongoing sintering and reaction processes and this is the reason why the RTP furnace modified for an in-situ resistance measurement was used. Other important advantages of using the RTP furnace were direct gas flow control and temperature control. The resistance was measured using four point method. Two molybdenum alloy probing wires were encapsulated in a ceramic guide jacket and contacts the paste spots on the substrate from the top. K-type thermocouples contacted the sample from the front and rear side to control the temperature during the process. The course of resistance was recorded for temperature above ca. 300 °C [7, 8, 10].

2. EXPERIMENTAL

2.1. Sample preparation

For this experiment were used (154 × 154 mm²) industrial N-type mono-Si substrates with crystallographic orientation [100], and with base resistivity ρ_{N-Si} in the range 2,5 - 3 Ω·cm. The saw damage removal was done in a sodium hydroxide (NaOH) solution, and the subsequently texturing in a solution of the mixture of potassium hydroxide (KOH) and hydrogen peroxide (H₂O₂). The emitter was created by atmospheric pressure diffusion using boron tribromide (BBr₃) as a source. The resulting sheet resistance of emitter was measured by four probe method and it was $R_{Sheet} = 75 \Omega / sq$ on the average. The emitter depth was measured using Electrochemical-Capacitance-Voltage measurement and it was ca. $d_{emitter} = 0.6 \mu m$. As the passivation and ARC coating an uniform 70 nm thick dielectric layer of SiO₂-SiN_x was deposited.

The experiment were used two commercially available pastes (named A and B) for fine-line front side metallization from various producers. The testing structure was created by 4 mm × 1 mm screen printed spots

at 50 mm distance. This structure was chosen due to simply positioning of measuring contacts. After the printing the wafers were dried at 200°C for 10 minutes.

2.2. Firing conditions

In this experiment were used two different temperature profiles, Profile 480 and Profile 400 (see the **Fig. 2**), which were varying in the first temperature U_H . In case of the Profile 480 the first temperature was set up to $U_H = 480$ °C with a heating rate 10 °C / sec. The second temperature was set up to $U_{peak} = 800$ °C with a heating rate 2 °C / sec. An immediate cooling then took place with a cooling rate of 10 °C / sec down to 100°C.

The Profile 400 differed from the Profile 480 in the first set up temperature $U_H = 400$ °C and in a heating rate, which was 8,33 °C / sec. The second temperature was set up to $U_{peak} = 800$ °C with a heating rate 2,5 °C / sec. The process of cooling was identical with the Profile 480.

The firing was done in an atmosphere of N_2 / O_2 gas mixture. The composition of the process gas was changed using an O_2 concentration between 21 % and 0 % keeping the total gas flow constant. The required concentration of O_2 was achieved by controlling the variation of the O_2 concentration in the N_2 atmosphere. The O_2 concentration at the first measurements for both profiles was coincident with the concentration in the atmosphere (21 % O_2). Afterwards it moved downwards to 10 %, to 5 %, and finally to 0 %. In case of the Profile 400 only the measurements with 21 % O_2 were done.

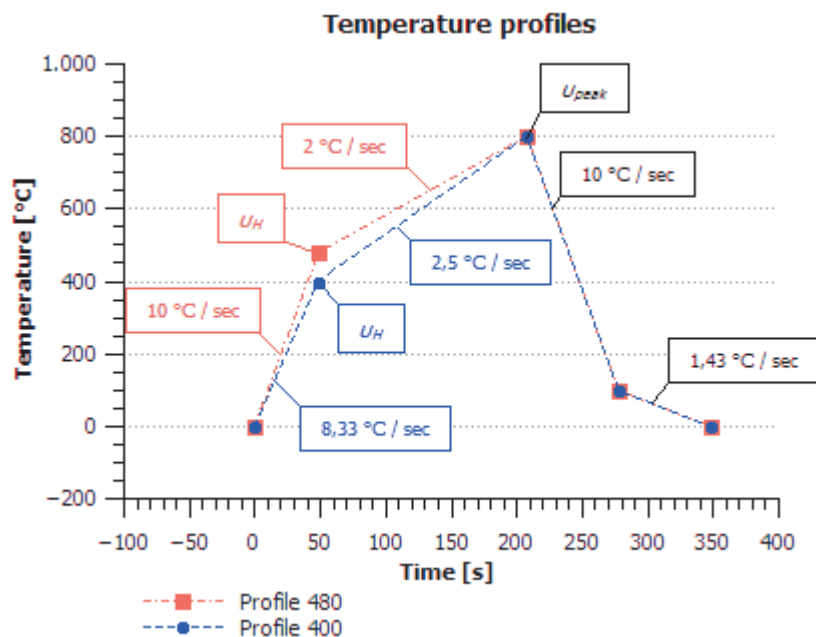


Fig. 2 Used temperature profiles

3. RESULTS AND DISCUSSION

The examples of resistance changes for Profile 480 are presented in the **Fig. 3** in case of paste A, or in the **Fig. 4** in case of paste B. The dependence of resistance on the temperature for both pastes in case of using Profile 400 is presented in the **Fig. 5**. From resistance dependence on temperature it is obvious that the resistance was alternating between conductive state and insulating state during firing. On the beginning there was no conductive connection between testing spots, because they were separated from the substrate by deposited SiO_2-SiN_x layer. The burning through the dielectric layer at temperature U_{BT} is indicated by the first conductive state, when melted glass is able to conduct current. The temperature U_{BT} is dependent of O_2 content in the process atmosphere and the temperature profile (see **Fig. 3**, **Fig. 4**, and **Fig. 5**).

Examples of resistance dependence on the temperature and the O₂ content are shown in the **Fig. 3**. It is evident, that at reduction of O₂ concentration the first insulating state became shorter and the temperature U_{BT} decreased from 525 °C (for 21 % O₂, **Fig. 3a**) to 519 °C (for 10 % O₂), to 513 °C (for 5 % O₂) and finally to 465 °C (for 0 % O₂, **Fig. 3b**). In case of paste B (see examples in the **Fig. 4**) the reduction in time of the first insulating state was more significant compared with paste A (**Fig. 3**). The reduction of O₂ concentration changed the temperature U_{BT} from 665 °C (for 21 % O₂, **Fig. 4a**) to 491 °C (for 10 % O₂), respective to 494 °C (for 5 % O₂) and finally to 398 °C (for 0 % O₂, **Fig. 4b**). Between 750 °C and 800 °C fluctuations occurred between insulating and conductive state in case of all samples. These fluctuations were most probably caused by reaction processes at the interface and formation of silver precipitates.

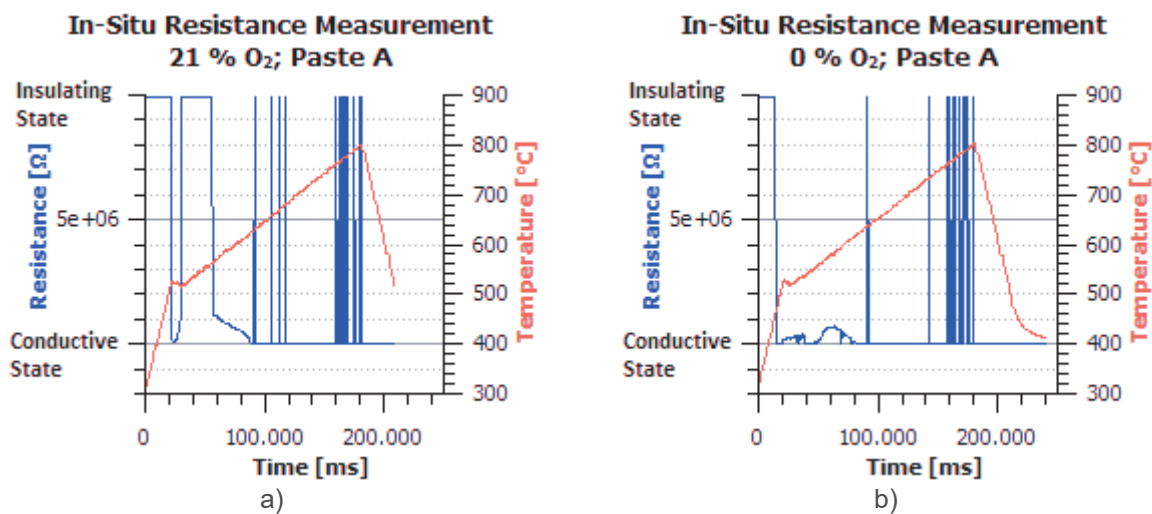


Fig. 3 The dependence of resistance on the temperature and the content of O₂ for the paste A

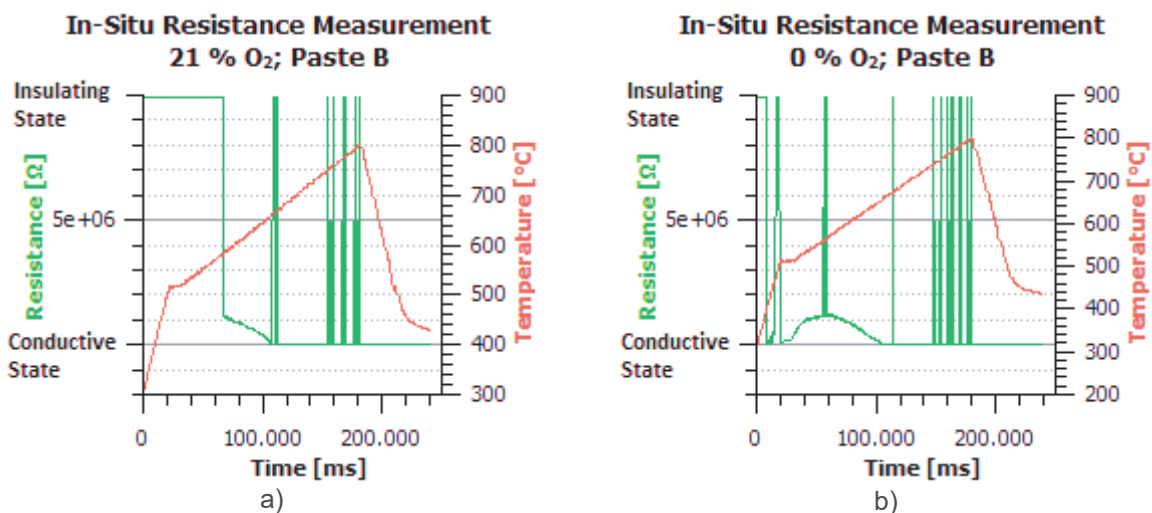


Fig. 4 The dependence of resistance on the temperature and the content of O₂ for the paste B

From the comparison of resistance dependence in the **Fig. 3a**) and in the **Fig. 5a**) (paste A), respectively the **Fig. 4a**) and the **Fig. 5a**) (paste B) it is obvious, that the reduction of the first target temperature U_H had a bigger impact on the resistance profile of the paste B. Time necessary to burning through the SiO₂-SiN_x layer became longer in both cases. Simultaneously the temperature U_{BT} decreased from 525°C to 480 °C for paste A, and from 665°C to 368 °C for paste B. Up to 630°C the paste B became conductive and no further insulating state was found.

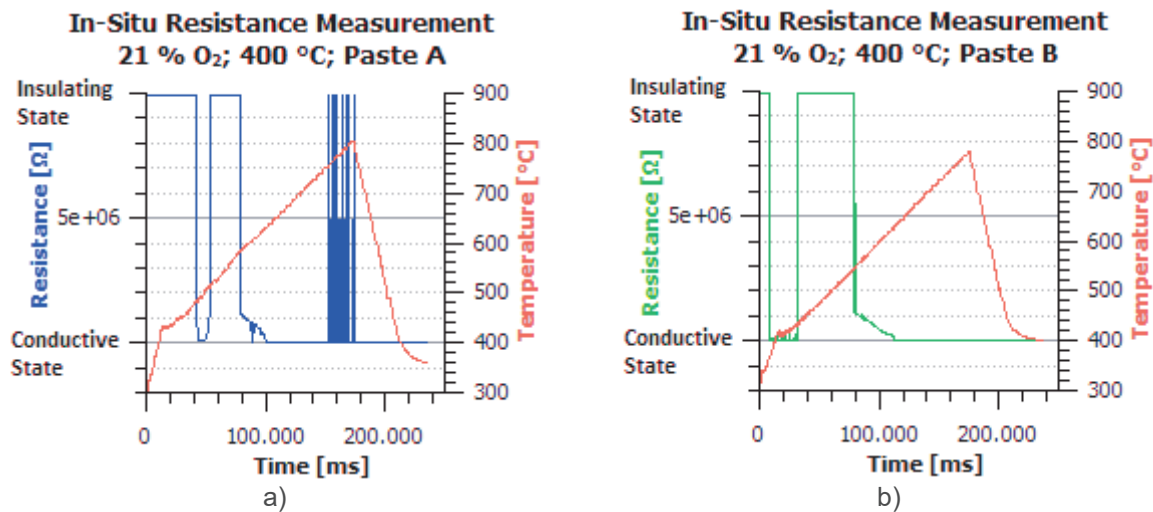


Fig. 5 The dependence of resistance on the temperature using Profile 400.

4. CONCLUSION

The contact formation of silver fine-line front side contacts screen printed on P⁺ doped Si with of SiO₂-SiN_x passivation layer was observed by in-situ contact resistance measurements. It is clear that in-situ resistance measurements proved to give insight in the kinetics of contact formation and showed differences in the contact formation process for different O₂ concentrations and temperature profiles. The temperature required for burning through the dielectric layer could be determined from the resistance profile.

The resistance profile of the paste B depended more on the O₂ content and the first target value u_H than the profile of the paste A. The temperature u_{BT} decreased by reduction of O₂ content from 525 °C to 465 °C in case of paste A, and from 665 °C to 398 °C in case of paste B. The reduction of the first target temperature u_H from 480 °C to 400 °C extended the time and decreased the temperature u_{BT} required for the burning through the ARC and passivation layer.

ACKNOWLEDGEMENTS

The article was supported by project no. FEKT-S-14-2300 A new types of electronic circuits and sensors for specific applications.

REFERENCES

- [1] DOBRZAŃSKI L. A., MUSZTYFAGA M., DRYGALA A., PANEK P. Investigation of the Screen Printed Contacts of Silicon Solar Cells Using Transmission Line Model. In Journal of Achievements in Materials and Manufacturing Engineering, Vol. 41, No. 1-2, 2010, pp. 57-65.
- [2] HÖRTEIS M. Fine-Line Printed Contacts on Crystalline Silicon Solar Cells. Fraunhofer Institut für Solare Energiesysteme: Freiburg im Breisgau, 2009.
- [3] MARTÍNEZ M. A. Low Temperature Processes for the Front-side Metallization of Crystalline Silicon Solar Cells. Fraunhofer Institut für Solare Energiesysteme: Freiburg im Breisgau, 2013.
- [4] EBERSTEIN M., SCHILM J., REINHARDT K., PARTSCH U. Kinetics Aspects of the Contact Formation by Glass Containing Silver Pastes. In 27th European Photovoltaics Solar Energy Conference and Exhibition. Frankfurt: 2012, pp. 840 - 844.
- [5] SCHUBERT G. Thick Film Metallization of Crystalline Silicon Solar Cells - Mechanism, Models and Applications. Universität Konstanz: Konstanz, 2006.
- [6] HONG K. K., CHO S. B., YOU J. S. Mechanism for the Formation of Ag Crystallites in the Ag Thick-film Contacts of Crystalline Si Solar Cells. In Solar Energy Materials and Solar Cells: 17th International Photovoltaic Science and Engineering Conference, Vol. 93, No. 6-7, 2009, pp. 898-904.

- [7] BALLIF C., HULJIĆ D. M., WILLEKE G., HESSLER-WYSER A. Silver Thick-film Contacts on Highly Doped N-type Silicon Emitters: Structural and Electronic Properties of the Interface. In Applied Physics Letters, Vol. 82, No. 12, pp. 1878-1880.
- [8] REINHARDT K., et al. Observation of the Contact Formation of PV Frontside Pastes by in-situ Contact Resistance Measurement. In Energy Procedia: Proceedings of the 4th International Conference on Crystalline Silicon Photovoltaic, Vol. 55, 2014, pp. 702-707.
- [9] BÄTZNER D. L., HANTON K., LI A., CUEVAS A. Investigation of the Co-firing Process for Contact Formation in Screen Printed Silicon Solar Cells. In 21st European Photovoltaic Solar Energy Conference. Dresden: 2006, pp. 807-810.
- [10] BUCK T., et al. Engineering and Characterization of Metal Contacts to P+ Doped Silicon. In 29th European Photovoltaics Solar Energy Conference and Exhibition. Amsterdam: 2014, pp. 401 - 405.